Landau levels, molecular orbitals, and the Hofstadter butterfly in finite systems

James G. Analytis, Stephen J. Blundell, and Arzhang Ardavan

Citation: American Journal of Physics **72**, 613 (2004); doi: 10.1119/1.1615568
View online: https://doi.org/10.1119/1.1615568
View Table of Contents: https://aapt.scitation.org/toc/ajp/72/5
Published by the American Association of Physics Teachers

Landau levels, molecular orbitals, and the Hofstadter butterfly in finite systems

James G. Analytis, Stephen J. Blundell,[a] and Arzhang Ardavan
Department of Physics, Clarendon Laboratory, University of Oxford, Parks Road, Oxford OX1 3PU, United Kingdom

(Received 3 June 2003; accepted 8 August 2003)

The Hofstadter butterfly is the energy spectrum of an infinite square lattice, plotted as a function of the magnetic field. We illustrate a method of calculating similar spectra for finite lattices in a magnetic field, using methods that consider the appropriate molecular orbitals, and find that the spectra resemble the Hofstadter butterfly. We relate the bonding and antibonding orbitals used to describe small systems to the Landau levels of the infinite system. This approach provides an unusual, but instructive, method of introducing the physics of Landau levels from the basic quantum mechanics of small systems. © *2004 American Association of Physics Teachers.*
[DOI: 10.1119/1.1615568]

I. INTRODUCTION

In the presence of a magnetic field, the electron energy states of a metal are quantized in Landau levels. A study of Landau levels leads to an understanding of phenomena such as the de Haas–van Alphen effect[1] and the quantum Hall effect.[2] Landau levels are traditionally introduced in solid state physics courses by considering infinite periodic systems. However, with the current interest in nanotechnology, quantum dots,[3] and single-molecule magnets,[4] it is useful to consider the opposite limit of a small bounded system. This limit is more suited to a molecular orbital description. In fact, chemists often are more familiar with thinking about the overlap of molecular orbitals than about tight-binding models, and for small systems the language of molecular orbitals is more appropriate. In this paper we show how we can consider the appearance of Landau levels and the emergence of the Hofstadter butterfly[5] in a small system. The approach naturally brings out the crossover between energy levels and energy bands and illustrates the effect of the magnetic field.

II. MOLECULAR ORBITALS IN ONE-DIMENSIONAL SYSTEMS

We begin by recalling results for the molecular orbitals in the hydrogen molecule H_2.[6] We label the component hydrogen atoms by A and B and express the wavefunction $|\psi\rangle$, which is a linear combination of atomic orbitals $|\psi_A\rangle$ and $|\psi_B\rangle$, as

$$|\psi\rangle = c_A|\psi_A\rangle + c_B|\psi_B\rangle. \tag{1}$$

Our Hamiltonian for one electron can be written as

$$\mathcal{H} = -\frac{\hbar^2}{2m}\nabla^2 + \mathbf{V}_A + \mathbf{V}_B, \tag{2}$$

where $\mathbf{V}_A$ and $\mathbf{V}_B$ denote the energy of attraction of an electron to each center. The diagonal integral, which can be approximated by the binding energy of the electron at one of the centers, is given by

$$E_0 = \langle\psi_A|\mathcal{H}|\psi_A\rangle, \tag{3}$$

and the resonance integral t by

$$t = \langle\psi_A|\mathcal{H}|\psi_B\rangle. \tag{4}$$

Equation (4) gives the energy of the electron when it resides in an overlap region between the centers. (In the language of solid-state physics, t is the transfer or hopping integral.)

In the simplest approximation (the Hückel approximation), the overlap integrals are given by $S_{ij} = \langle\psi_i|\psi_j\rangle = \delta_{ij}$. Hence, the secular equation $|H_{ij} - ES_{ij}| = 0$ can be written as

$$\begin{vmatrix} E_0 - E & t \\ t & E_0 - E \end{vmatrix} = 0, \tag{5}$$

with solutions

$$E = E_0 \pm t. \tag{6}$$

The corresponding eigenfunctions are the bonding (σ) and antibonding (σ^*) molecular orbitals in hydrogen[6,7] and are illustrated in Fig. 1(a). We take $t<0$ so that the bonding state (which has $c_A = c_B$) has a lower energy than the antibonding state. The hydrogen molecule has two electrons so the σ level is full and the σ^* level is empty. The extension to a six-membered ring (such as benzene) is straightforward and yields three bonding (a and e) and three antibonding (a^* and e^*) molecular orbitals [see Fig. 1(b)]. Benzene has six electrons participating in bonding, so all the bonding orbitals will be full and all the antibonding orbitals will be empty.[6]

A. Linear chain

We can find the energy levels for a linear chain by extending Eq. (5) so that only nearest neighbor interactions are included. For a linear chain of N atoms, the equation to solve is

$$\begin{vmatrix} E_0 - E & t & 0 & 0\cdots 0 & 0 \\ t & E_0 - E & t & 0\cdots 0 & 0 \\ 0 & t & E_0 - E & t\cdots 0 & 0 \\ \vdots & \vdots & \vdots & \vdots\ddots\vdots & \vdots \\ 0 & 0 & 0 & 0\cdots E_0 - E & t \\ 0 & 0 & 0 & 0\cdots t & E_0 - E \end{vmatrix} = 0, \tag{7}$$

which has solutions[8]

$$E = E_0 - 2|t|\cos\left(\frac{\pi M}{N+1}\right), \tag{8}$$

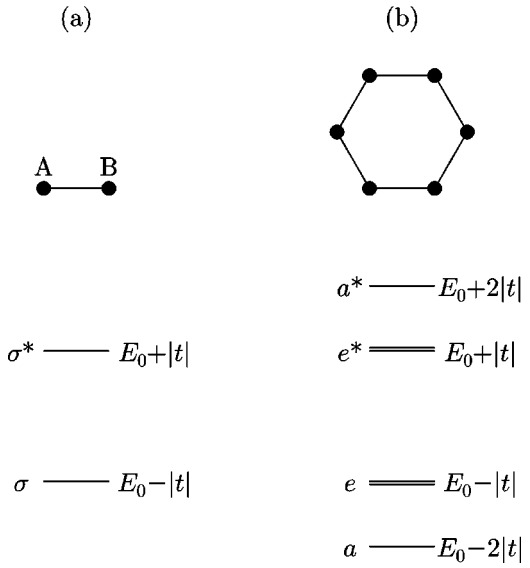

Fig. 1. Molecular orbitals in (a) H_2 and (b) benzene.

where $M=1,2,\ldots,N$. Figure 2(a) depicts the energy levels of a linear chain as the atoms increase in number. There are as many energy levels as there are atoms and each energy level is nondegenerate. The case of $N=2$ is, of course, that of hydrogen and is identical with that shown in Fig. 1(a). As $N\to\infty$, we recover the one-dimensional tight-binding band, familiar from undergraduate courses on solid-state physics.[9] The bandwidth approaches $4|t|$ as $N\to\infty$, which is the result for the one-dimensional tight-binding band.

B. Polygonal chain

It is also possible to solve the problem of the chain of N atoms, with the two ends joined, so that it becomes a polygon, as illustrated in the inset to Fig. 2(b). In this case, we solve

$$\begin{vmatrix} E_0-E & t & 0 & 0\cdots 0 & t \\ t & E_0-E & t & 0\cdots 0 & 0 \\ 0 & t & E_0-E & t\cdots 0 & 0 \\ \vdots & \vdots & \vdots & \vdots\ddots\vdots & \vdots \\ 0 & 0 & 0 & 0\cdots E_0-E & t \\ t & 0 & 0 & 0\cdots t & E_0-E \end{vmatrix} = 0, \tag{9}$$

in which the only difference from Eq. (7) is the terms on the bottom-left and top-right corners of the determinant. In this case the solutions are

$$E=E_0-2|t|\cos\left(\frac{2\pi M}{N}\right), \tag{10}$$

where $M=1,2,\ldots,N$. Figure 2(b) depicts these energy levels. In this case, each energy level is doubly degenerate, except for the singly degenerate bonding level at $E=E_0-2|t|$ (which exists for all N) and the singly-degenerate antibonding level at $E=E_0+2|t|$ (which exists for even N). The case

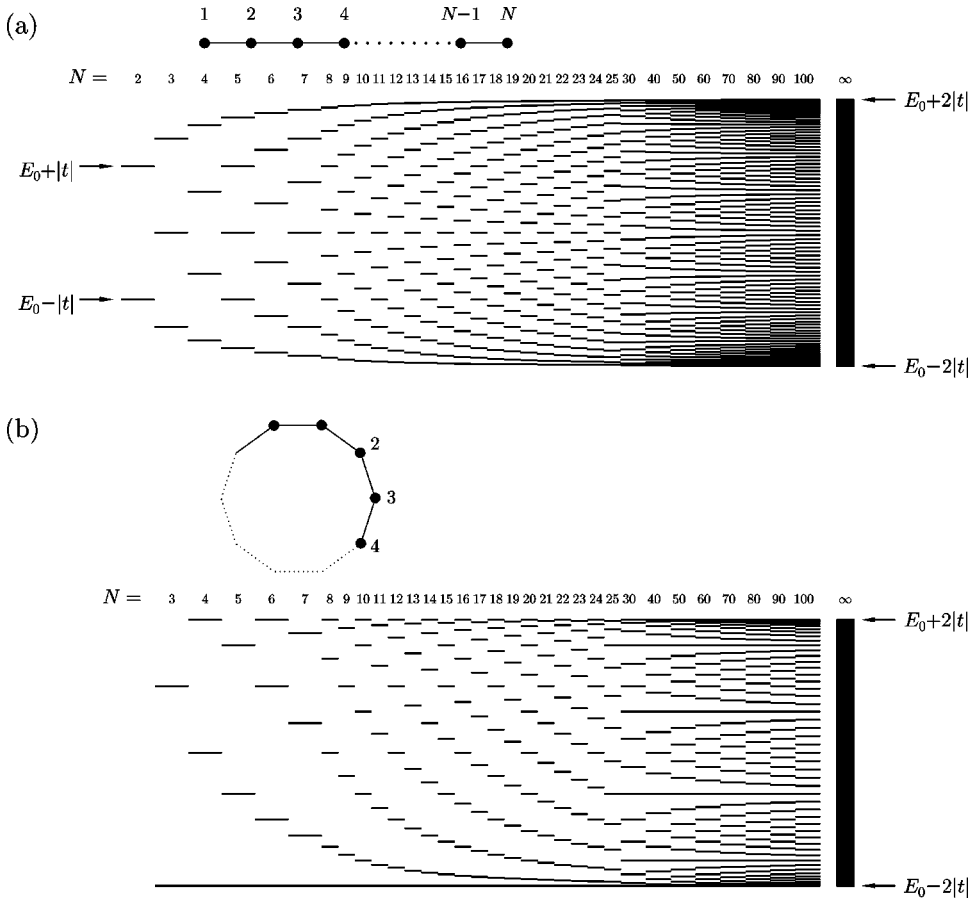

Fig. 2. Energy levels for molecular orbitals in (a) a one-dimensional chain and (b) a polygon. As the number of atoms, $N\to\infty$, the energy levels become a continuum.

of $N=6$ is that of benzene and is identical with that shown in Fig. 1(b).

Because of the higher symmetry of the polygon (compared with the chain), the molecular orbitals can be found more easily because every site is symmetrically related. If we write the wave function of the nth site as ψ_n, this symmetry implies that $\psi_n = e^{i\phi}\psi_{n-1}$ (Bloch's theorem[9–11]). We need to solve

$$\mathcal{H}\psi_n = E\psi_n = -|t|\psi_{n-1} - |t|\psi_{n+1} + E_0\psi_n, \tag{11}$$

and hence $E = E_0 - 2|t|\cos\phi$. Because $\psi_{N+1} = \psi_1$, we have that $e^{iN\phi} = 1$, and hence $\phi = 2\pi M/N$, so that Eq. (10) follows immediately. As for the case of the linear chain, the limit $N \to \infty$ recovers the one-dimensional tight-binding band.

III. THE EFFECT OF A STATIC MAGNETIC FIELD

We now consider the effect of a magnetic field. Recall that the momentum $\mathbf{p}$ operator generates a translation operator[12] given by

$$\hat{T}(\mathbf{L}) = \exp\left(\frac{i}{\hbar}\mathbf{p}\cdot\mathbf{L}\right). \tag{12}$$

Hence $\psi(\mathbf{r}+\mathbf{L}) = \hat{T}(\mathbf{L})\psi(\mathbf{r})$.

If we add a magnetic field, the momentum operator $\mathbf{p}$ is replaced by an operator that includes the magnetic vector potential $\mathbf{A}$,

$$\mathbf{p} \to \mathbf{p} + e\mathbf{A}, \tag{13}$$

which is known as the Peierls substitution.[13] Thus, the effect of the magnetic field is to introduce an extra phase factor into a translated wave function, so that

$$\psi(\mathbf{r}+\mathbf{L}) = \exp\left(\frac{ie}{\hbar}\int_{\mathbf{r}}^{\mathbf{r}+\mathbf{L}} \mathbf{A}\cdot d\mathbf{l}\right)\hat{T}(\mathbf{L})\psi(\mathbf{r}), \tag{14}$$

where $\hat{T}(\mathbf{L})$ is the translation operator [Eq. (12)] in the absence of a magnetic field.

In particular, if the path along which we translate is closed, the wave function gains a phase of the form

$$\exp\left(\frac{ie}{\hbar}\oint \mathbf{A}\cdot d\mathbf{l}\right) = \exp\left(2\pi i\frac{\Phi}{\Phi_0}\right), \tag{15}$$

where $\Phi = \int \mathbf{B}\cdot d\mathbf{S}$ is the magnetic flux enclosed by the path and $\Phi_0 = h/e$ is the flux quantum. This phase factor gives rise to the well-known Aharonov–Bohm effect.[14] In the rest of this paper we will define α to be the number of flux quanta passing through a closed path, that is,

$$\alpha \equiv \frac{\Phi}{\Phi_0}, \tag{16}$$

so that the phase factor of Eq. (15) can be written as $e^{2\pi i\alpha}$. We illustrate this result for two simple cases.

A. Free particle on a circular ring

Consider a free, spinless particle (mass m, charge $-e$) confined to a circular ring of radius $r=a$, lying in the xy plane. The Hamiltonian for this particle can be written as

$$\mathcal{H} = -\frac{\hbar^2}{2m}\frac{1}{r^2}\frac{\partial^2}{\partial\phi^2}, \tag{17}$$

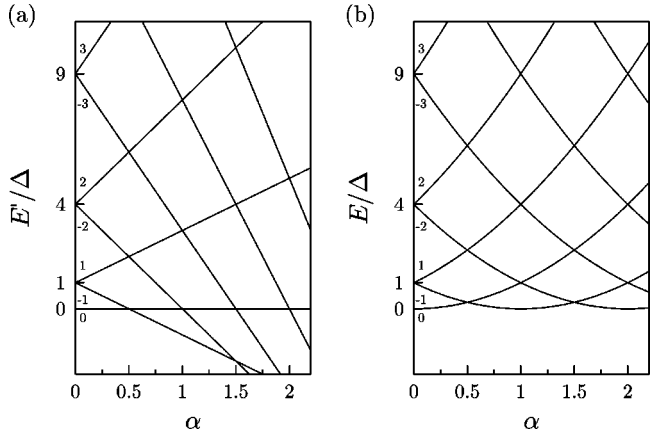

Fig. 3. The energy spectrum for a free particle on a ring in a magnetic field. (a) $E' = E - e^2B^2a^2/8m$ as a function of α. (b) E as a function of α. In each plot, $\Delta = \hbar^2/2I$ and each level is labeled by the value of M.

where ϕ is the angle around the ring. The energy eigenvalues are therefore given by $E = \hbar^2M^2/2I$, where $I = ma^2$ is the moment of inertia of the particle about the axis of the ring, and $M = 0, \pm 1, \pm 2, \ldots$. The energy eigenfunctions are $\psi_M = e^{iM\phi}$ and are simultaneously eigenstates of the angular momentum operator $\hat{L}_z = -i\hbar\partial/\partial\phi$ with eigenvalues $\hbar M$.

We now apply a magnetic field $\mathbf{B} = B\hat{\mathbf{z}}$ perpendicular to the ring. If we write the magnetic vector potential as

$$\mathbf{A} = \frac{1}{2}\mathbf{B}\times\mathbf{r} = \frac{B}{2}(-y,x,0) = \frac{Ba}{2}\hat{\boldsymbol{\phi}}, \tag{18}$$

the additional phase factor due to the magnetic field for a rotation of angle ϕ is therefore

$$\exp\left(\frac{ie}{\hbar}\frac{Ba^2\phi}{2}\right) = e^{i\alpha\phi}, \tag{19}$$

where the flux through the ring is $\Phi = B\pi a^2$. Hence, the energy eigenfunctions become $\psi_M = e^{i(M+\alpha)\phi}$ with energy eigenvalues

$$E = \frac{\hbar^2}{2I}(M+\alpha)^2. \tag{20}$$

The bracket in Eq. (20) can be expanded, yielding

$$E = \frac{\hbar^2}{2I}M^2 + M\mu_B B + \frac{e^2B^2a^2}{8m}, \tag{21}$$

where $\mu_B = e\hbar/2m$ is the Bohr magneton.

The first term in Eq. (21) is field independent and represents the angular kinetic energy. The second term in Eq. (21) represents the paramagnetic response of energy levels with different angular momenta $M\hbar$. The first two terms are plotted in Fig. 3(a) and illustrate how the magnetic field splits each $\pm M$ doublet by an amount proportional to $|M|$ (the Zeeman effect). The third term in Eq. (21) is the diamagnetic response (always positive and proportional to B^2)[15] and when included produces the spectra shown in Fig. 3(b). As required, these spectra are periodic in α, so that if there is exactly a whole number of flux quanta through the ring, the energy spectra are identical to the zero-field case.[16] Because the energy eigenfunctions have angular momentum $L_z = \hbar(M+\alpha)$, they each correspond to a state in which the

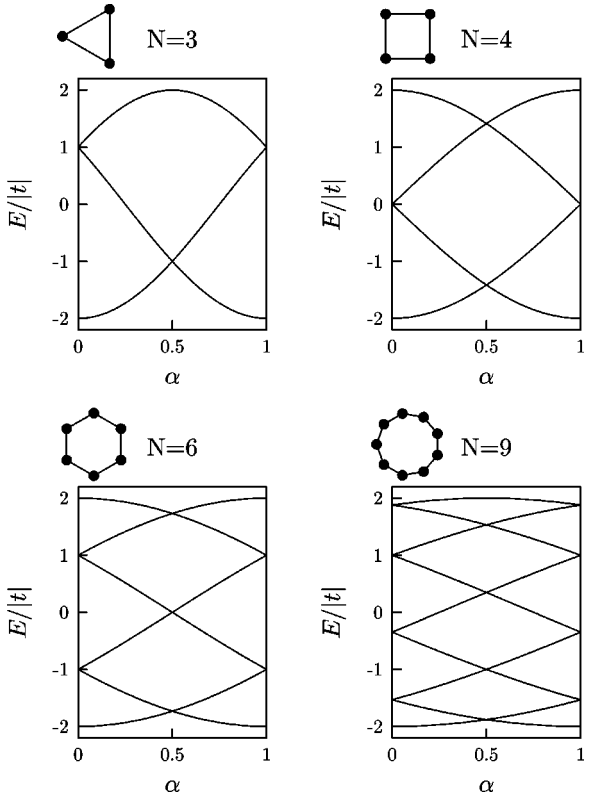

Fig. 4. The energy spectrum for the molecular orbitals on a polygon for different values of N.

electron travels around the ring with angular velocity $\Omega = L_z/I$. Hence, each energy eigenfunction can be associated with a persistent current[17] $I_{\text{persistent}}$, given by

$$I_{\text{persistent}} = (-e)\frac{\Omega}{2\pi} = -\frac{e\hbar}{2\pi m r^2}(M+\alpha). \tag{22}$$

B. Particle on a tight-binding polygonal chain

We return to the molecular orbitals of the polygon considered in Sec. II B. With a magnetic field perpendicular to the polygon, we need to solve

$$\mathcal{H}\psi_n = E\psi_n = -|t|e^{-2\pi i\alpha/N}\psi_{n-1} - |t|e^{2\pi i\alpha/N}\psi_{n+1} + E_0\psi_n, \tag{23}$$

where α is the number of flux quanta threading the polygon. Hence, with $\psi_{N+1} = e^{2\pi i\alpha}\psi_1$, we have $E = E_0 - 2|t|\cos\phi$ and $\phi = 2\pi(M+\alpha)/N$. The energy eigenvalues are given by

$$E = E_0 - 2|t|\cos\left(\frac{2\pi}{N}(M+\alpha)\right). \tag{24}$$

These results are illustrated in Fig. 4. Without loss of generality, we take $E_0 = 0$ in this and subsequent plots, because this parameter simply defines the effective on-site energy and is thus an additive constant.

Figure 4 shows that the doublets in the zero-field energy spectra are split by the magnetic field in a manner reminiscent of that in Fig. 3(b). The lowest bonding level ($M=0$) also has the upward, initially quadratic, curvature, typical of a diamagnetic response, as found for the lowest level in Fig. 3(b). Once again, the levels can be labeled by their angular momenta (for example, for $N=6$ the levels are $0, -1, 1, -2, 2, 3$ in order of increasing energy near $\alpha = 0$), because the rotational symmetry makes the angular momentum a good quantum number. However, because of the tight-binding dispersion, the energy spectra are bounded in energy (the maximum dispersion is $4|t|$). Moreover, there is a noticeable difference between the cases of odd and even N: even N yields spectra which are symmetric about reflection in the line $E/|t| = 0$.

IV. FINITE LATTICES

In Sec. III B, the magnetic-field dependence of tight-binding networks was deduced, but each of the networks considered there were topologically identical to a ring. We now want to extend this analysis to tight-binding networks consisting of finite sections of a square lattice with lattice spacing a. This type of approach has been useful in studying quantum dot arrays.[18,19]

We write the wave function at site $(x,y) = (ma, na)$ as $\psi_{m,n}$, and thus the only nonzero matrix elements of the Hamiltonian are

$$\langle \psi_{m,n}|H|\psi_{m,n\pm1}\rangle = t, \tag{25}$$

$$\langle \psi_{m,n}|H|\psi_{m\pm1,n}\rangle = t, \tag{26}$$

and

$$\langle \psi_{m,n}|H|\psi_{k,l}\rangle = E_0\delta_{mk}\delta_{nl}. \tag{27}$$

As before, we can include the magnetic-field dependence of the energy spectra using Eq. (14). If we take $\mathbf{A} = (0, Bx, 0)$ without loss of generality, Eqs. (25) and (26) become

$$\langle \psi_{m,n}|H|\psi_{m,n\pm1}\rangle = te^{\pm 2\pi i m\alpha}, \tag{28}$$

$$\langle \psi_{m,n}|H|\psi_{m\pm1,n}\rangle = t, \tag{29}$$

where $\alpha = Ba^2/\Phi_0$, the number of flux quanta passing through each plaquette. Each plaquette of the lattice therefore contributes an Aharonov–Bohm phase factor $e^{2\pi i\alpha}$. A routine diagonalization procedure allows us to calculate the spectra for finite lattices with increasing numbers of plaquettes. The energy eigenvalues for this Hamiltonian can therefore be calculated numerically as a function of the magnetic field and the results are shown in Fig. 5.

Figure 5(a) shows the energy spectra for a lattice with $4 = 2\times 2$ sites, and is, of course, identical to the plot of the energy spectra for an $N=4$ polygon in Fig. 4. Figure 5(b) is for $9 = 3\times 3$ sites; at $B=0$ there are nine levels, consisting of two levels of single degeneracy, two of double degeneracy, and one nonbonding ($E=0$) level of triple degeneracy. For 16 sites [Fig. 5(c)], there are 16 levels at $B=0$, consisting of four levels of single degeneracy, four of double degeneracy, and one nonbonding level of quadruple degeneracy. These levels move in rather complex ways as the field B increases from zero. Figures 5(d)–5(f) show more complex behavior for larger numbers of sites. At $B=0$ there are now 36, 49, or 100 levels for Figs. 5(d), 5(e), and 5(f), respectively, and the nonbonding level at $E=0$ has degeneracies 6, 7, and 10, respectively. If there are an odd number of sites in the lattice, there will always be one nonbonding orbital that persists for all α. For a lattice with an even number of sites, the energy levels repeatedly cross the line $E=0$ as a function of α.

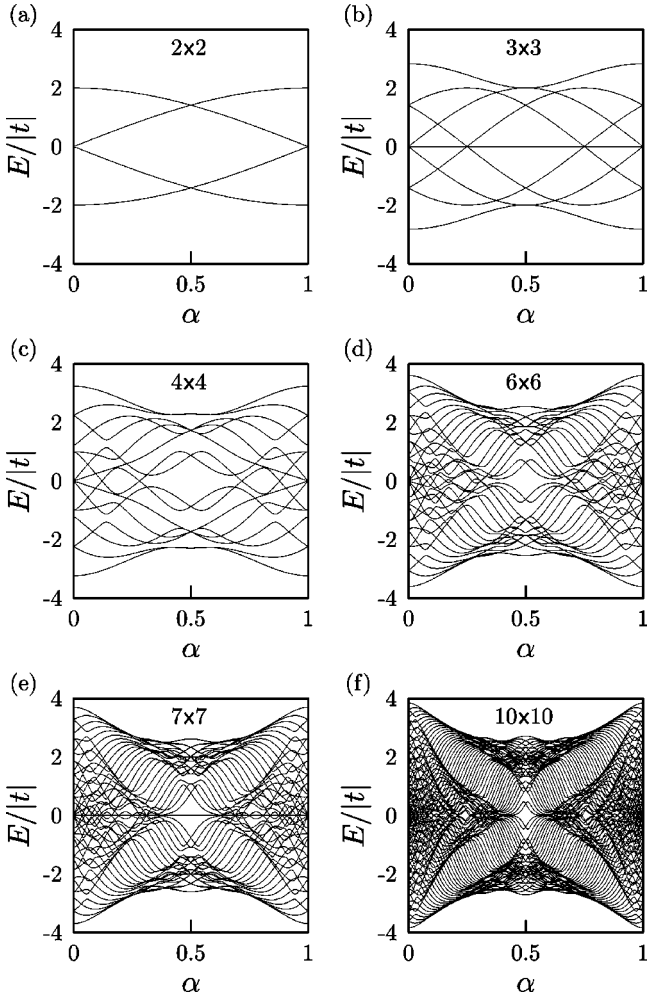

Fig. 5. Energy spectra for finite sections of a square lattice with (a) $4=2\times2$ sites, (b) $9=3\times3$ sites, (c) $16=4\times4$ sites, (d) $36=6\times6$ sites, (e) $49=7\times7$ sites, and (f) $100=10\times10$ sites.

The bandwidth is $4|t|$ for 4 sites [Fig. 5(b)], the result for the one-dimensional tight-binding band, but approaches $8|t|$ as the number of sites increases, which is the value for the two-dimensional tight-binding band. This latter result can be obtained as follows: the tight-binding model for an infinite two-dimensional square lattice yields an energy dispersion $E(\mathbf{k})$, given by[9]

$$E(\mathbf{k})=-2|t|(\cos(k_x a)+\cos(k_y a)), \tag{30}$$

which means that the allowed energies are $-4|t|\leqslant E\leqslant 4|t|$, and hence the bandwidth is $8|t|$.

In the presence of a magnetic field, the energy spectrum for the infinite two-dimensional square lattice is that of the Hofstadter butterfly,[5] which is shown in Fig. 6. This remarkable spectrum has a self-similar structure and is a fractal. When $\alpha=p/q$ (p, q integers) the spectrum comprises q Landau sub-bands and hence the spectrum has a very intricate dependence on magnetic field. The spectra plotted in Fig. 5 demonstrate that as the size of a finite system increases, the appearance of the spectra with many sites begins to approach that of the Hofstadter butterfly. In fact, a pattern that resembles the Hofstadter butterfly can be discerned for fairly small lattice sizes (see Fig. 5), but with one important difference. The finite lattices have energies available where they are forbidden in the infinite case. These energies are sparse and nondegenerate. Conversely, energies that correspond to available states in the Hofstadter butterfly are dense and highly degenerate. We can therefore see that the structure of broadened Landau levels in the Hofstadter butterfly emerge in finite systems.

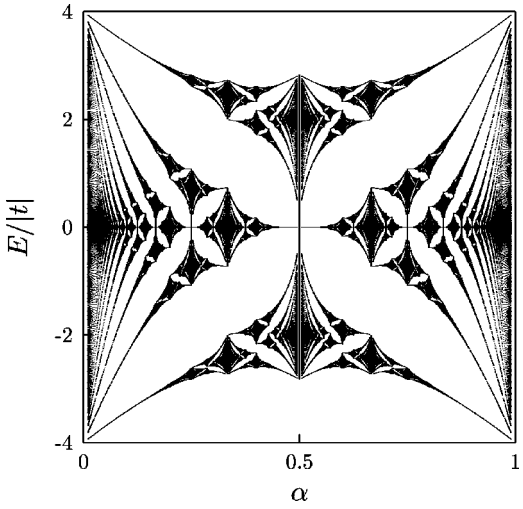

Fig. 6. Hofstadter's Butterfly for an infinite two-dimensional square lattice with tight-binding dispersion. This dispersion was first obtained by Hofstadter (Ref. 5).

V. DISCUSSION

In solid-state physics, the behavior of electrons in magnetic fields is usually introduced using the Hamiltonian

$$\mathcal{H}=\frac{1}{2m}(\mathbf{p}+e\mathbf{A})^2. \tag{31}$$

If we write $\boldsymbol{\pi}=(\mathbf{p}+e\mathbf{A})/\sqrt{eB\hbar}$, and choose the gauge $\mathbf{A}=\frac{1}{2}\mathbf{B}\times\mathbf{r}$, we can show that the commutator $[\pi_x,\pi_y]=-i$, and, hence,

$$\dot{\pi}_x=\frac{1}{i\hbar}[\pi_x,\mathcal{H}]=-\omega_c\pi_y, \tag{32a}$$

$$\dot{\pi}_y=\frac{1}{i\hbar}[\pi_y,\mathcal{H}]=\omega_c\pi_x, \tag{32b}$$

where $\omega_c=eB/m$ is the cyclotron frequency. Hence, the problem is equivalent to a simple harmonic oscillator, and the energy eigenvalues are

$$E=(n+\tfrac{1}{2})\hbar\omega_c, \tag{33}$$

and the energy eigenfunctions are known as Landau levels.[11,15,20–22]

This treatment is for free electrons, but near the bottom of the two-dimensional tight-binding band [Eq. (30)], the energy is approximately free-electron-like,

$$E(\mathbf{k})\approx-4|t|+\frac{\hbar^2}{2m^*}(k_x^2+k_y^2), \tag{34}$$

where the effective mass $m^*=\hbar^2/(2|t|a^2)$. Hence, the cyclotron frequency is

$$\omega_c=\frac{eB}{m^*}=\frac{4\pi\alpha|t|}{\hbar}, \tag{35}$$

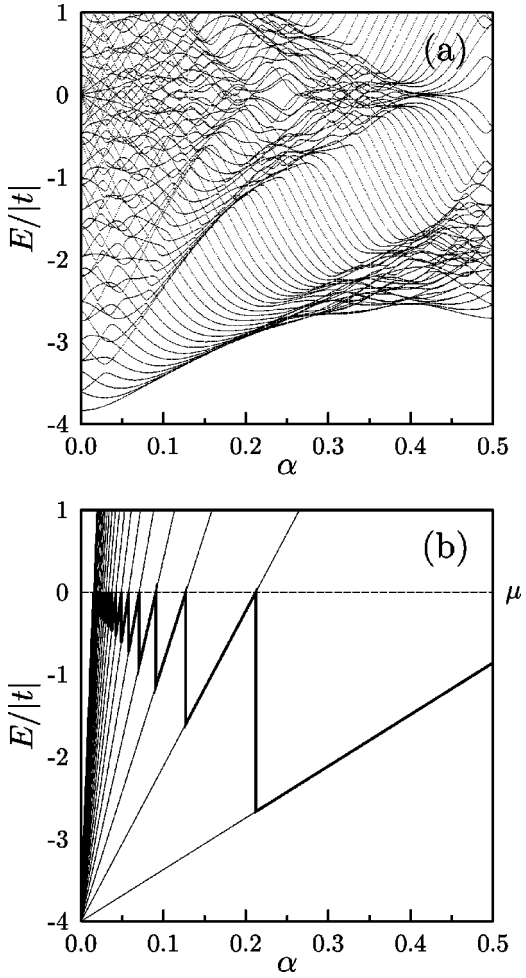

Fig. 7. A comparison of (a) the spectrum for the section of square lattice with 10×10 sites [an enlargement of Fig. 5(f)], and (b) the fan of Landau levels according to Eq. (36). The chemical potential μ has been set to zero for the case of a half-filled band.

and therefore the Landau levels near the bottom of the band can be written as

$$\frac{E}{|t|}=-4+4\pi\alpha\left(n+\frac{1}{2}\right). \tag{36}$$

In Fig. 7 we compare the spectrum of a small section of square lattice with 10×10 sites [Fig. 7(a)] with the fan of Landau levels given by Eq. (36) plotted in Fig. 7(b). The fan of Landau levels can be clearly seen emerging from the pattern in Fig. 7(a).

It is this fan of Landau levels that is responsible for the de Haas–van Alphen and the Shubnikov–de Haas effects.[1,11,15,20–22] In these effects occupied Landau levels cross the chemical potential μ and the Fermi energy E_F drops to the next highest Landau level [Fig. 7(b)]. In a similar way, the energy of the bonding orbitals of the finite systems increases in the dense regions and rapidly drops in the sparse regions [Fig. 7(a)]. These orbitals thus exhibit the essential features of magnetic oscillations in two-dimensional systems.

VI. CONCLUSIONS

The Hofstadter butterfly is the energy spectrum of an infinite square lattice in the presence of a perpendicular magnetic field. Using molecular orbital methods, we have shown how the energy spectra of finite sections of a square lattice approach this behavior as their size increases. For small systems, the appropriate description is in terms of bonding and antibonding orbitals, and we have shown how these orbitals become Landau levels in the limit of infinite system size. This approach provides an unusual, but instructive, method of introducing the physics of Landau levels from the quantum mechanics of small systems.

ACKNOWLEDGMENT

The authors would like to thank Dr. A. Coldea for useful discussions.

[a)]Electronic mail: s.blundell@physics.ox.ac.uk

[1]D. Shoenberg, *Magnetic Oscillations in Metals* (Cambridge University Press, Cambridge, 1986).
[2]R. E. Prange and S. M. Girvin, *The Quantum Hall Effect* (Springer-Verlag, New York, 1990); H. Aoki, "Quantised Hall effect," Rep. Prog. Phys. **50**, 655–730 (1987).
[3]A. P. Alivisatos, "Semiconductor clusters, nanocrystals and quantum dots," Science **271**, 933–937 (1996).
[4]W. Wernsdorfer, "Classical and quantum magnetization reversal studied in nanometer-sized particles and clusters," Adv. Chem. Phys. **118**, 99–190 (2001).
[5]D. R. Hofstadter, "Energy levels and wave functions of Bloch electrons in rational and irrational magnetic fields," Phys. Rev. B **14**, 2239–2249 (1976).
[6]P. W. Atkins and R. S. Friedman, *Molecular Quantum Mechanics*, 3rd ed. (Oxford University Press, Oxford, 1997), Chap. 8.
[7]Bonding levels provide a net lowering of the energy and have energy $<E_0$. Antibonding levels provide a net raising of the energy and have energy $>E_0$. Nonbonding levels have energy $=E_0$.
[8]C. A. Coulson, "The electronic structure of some polyenes and aromatic molecules. IV. The nature of the links of certain free radicals," Proc. R. Soc. London, Ser. A **164**, 383–396 (1938).
[9]C. Kittel, *Introduction to Solid State Physics*, 7th ed. (Wiley, New York, 1996).
[10]S. L. Altmann, *Band Theory of Solids: An Introduction From the Point of View of Symmetry* (Oxford University Press, Oxford, 1991).
[11]J. Singleton, *Band Theory and Electronic Properties of Solids* (Oxford University Press, Oxford, 2001).
[12]L. D. Landau and E. M. Lifshitz, *Quantum Mechanics*, 3rd ed. (Pergamon, Oxford, 1977), p. 45.
[13]R. E. Peierls, *Quantum Theory of Solids* (Oxford University Press, Oxford, 1955), p. 145.
[14]Y. Aharonov and D. Bohm, "Significance of electromagnetic potentials in quantum theory," Phys. Rev. **115**, 485–491 (1955); A. Shapere and F. Wilczek, *Geometric Phases in Physics* (World Scientific, Singapore, 1989).
[15]S. Blundell, *Magnetism in Condensed Matter* (Oxford University Press, Oxford, 2001).
[16]N. Byers and C. N. Yang, "Theoretical considerations concerning quantized magnetic flux in superconducting cylinders," Phys. Rev. Lett. **7**, 46–49 (1961).
[17]H.-F. Cheung, Y. Gefen, E. K. Riedel, and W.-H. Shih, "Persistent currents in small one-dimensional metal rings," Phys. Rev. B **37**, 6050–6062 (1988).
[18]U. Sivan, Y. Imry, and C. Hartzstein, "Ahranov–Bohm and quantum Hall effects in singly connected quantum dots," Phys. Rev. B **39**, 1242–1250 (1989).
[19]R. Kotlyar, C. A. Stafford, and S. Das Sarma, "Addition spectrum, persistent current, and spin polarization, in coupled quantum dot arrays: coherence, correlation and disorder," Phys. Rev. B **58**, 3989–4013 (1998).
[20]C. Kittel, *Quantum Theory of Solids* (Wiley, New York, 1963).
[21]J. H. Davies, *The Physics of Low-Dimensional Semiconductors* (Cambridge University Press, Cambridge, 1998).
[22]L. D. Landau and E. M. Lifshitz, *Quantum Mechanics*, 3rd ed. (Pergamon, Oxford, 1977), pp. 456–458.